Phase-Type Gratings Formed by Photochemical Phase Transition of Polymer Azobenzene Liquid Crystals: Enhancement of Diffraction Efficiency by Spatial Modulation of Molecular Alignment

Takahiro Yamamoto, Makoto Hasegawa, Akihiko Kanazawa, Takeshi Shiono, and Tomiki Ikeda*

Research Laboratory of Resources Utilization, Tokyo Institute of Technology, 4259 Nagatsuta, Midori-ku, Yokohama 226−8503, Japan

Received: June 28, 1999

Unique characteristics were observed in phase-type gratings that were formed in a polymer azobenzene liquid-crystal (PALC) film. Generation of sinusoidal variation of the surface of the film was confirmed by atomic force microscopy. However, comparison of the diffraction efficiency with the surface modulation revealed that the gratings could not be characterized only as conventional surface-relief gratings. In the glassy state of the film, moderate efficiency (∼18%) was obtained with large surface modulation (68−76 nm), whereas the gratings recorded in the nematic (N) phase showed high diffraction efficiency (∼28%) with slight surface modulation (33−53 nm). The diffraction efficiency was enhanced in the liquid-crystalline phase. Dynamics of the first-order diffraction beam exhibited that the grating formation was associated with photochemical phase transition of PALC. It was assumed that the isotropic (I) phases were formed by photochemical reaction of azobenzene moieties in the interference pattern at an appropriate interval. The grating would be made up by alternate arrangement of the I and the N phases as well as slight modulation of surface structure. Our speculation was supported by atomic force and polarizing optical microscopy. Anisotropy in the diffraction efficiency with respect to the linearly polarized readout beam also supported our hypothesis. It was revealed that the large enhancement of the efficiency was attributable to spatial modulation of molecular alignment.

Introduction

Recently, intensive research activities have been directed toward development of materials for holography due to scientific and industrial interest. Holography is the image-storage process that is radically different from other methods: both phase and amplitude of wave fields that intersect on a recording medium are recorded. This method is expected to be a promising candidate for storage of high-density information as well as recording of three-dimensional (3-D) objects. Since Todorov and co-workers reported optically induced birefringence of azobenzene groups in a variety of polymer matrices,[1] numerous research groups have concentrated on exploration of materials with high diffraction efficiency, resolution, and sensitivity.[2−12] Among those materials, polymers functionalized with azobenzenes seem to be the most suitable material for holographic storage. In recording phase-type holograms, light-induced large modulations in either surface structure or refractive index are necessary to acquire high efficiency. In fact, Wendorff and co-workers performed the recording of birefringence gratings with high diffraction efficiency and the storage of real 3-D objects by means of polymer liquid crystals (PLCs) containing azobenzene moieties.[7]

Liquid crystals (LCs) are typical self-organizing materials with unique and excellent properties such as (1) a self-organizing nature at certain temperature range with fluidity and long-range order, (2) a cooperative effect, (3) a large optical anisotropy, and (4) an alignment change by an external field at surface and interface. Owing to these excellent properties, LC materials are expected to be used not only in liquid crystal displays but also in various photonic applications. The large optical anisotropy is especially favorable for fabrication of phase-type gratings with high efficiencies.

Photonics, in which properties of light are controlled by a stimulating light, has become of interest as a future technology because of advantages in high-speed information processing. To establish the LC materials for photonics, we have paid much attention to photochemical reaction of azobenzene derivatives. For instance, azobenzene derivatives in a trans form are rodlike, which tends to stabilize the phase structure of liquid-crystalline phases. However, cis forms are bent and destabilize the phase structure and lower clearing temperature. Furthermore, it is known that some azobenzene derivatives show liquid-crystalline properties. We have performed so far studies on photochemical control of LC materials containing a variety of azobenzene derivatives.[13] We already reported the optical switching by transmission-,[13a−d] reflection-,[13e,f] and scattering-mode[13g] analyses. For example, rapid optical switching of a transmitted probe beam through crossed polarizers could be achieved with light as a stimulus. In addition, we succeeded in storing two-dimensional images into PLCs functionalized with azobenzenes.[13a] The photochemical phase transition produces a large change in refractive index in LC materials, which is obviously advantageous to control of light waves.

In the past decade, direct formation of gratings by inscribing the surface of azobenzene polymer films has extensively been explored.[3b,8,9] All of the polymers reported had high glass-transition temperatures (T_g > 100 °C), and hence, stored information was fairly stable at room temperature. This feature is favorable to the application of polymers to recording materials. In these studies, however, the effects of photoinduced modula-

* To whom correspondence should be addressed. Phone: 81-45-924-5240. FAX: 81-45-924-5275. E-mail: tikeda@res.titech.ac.jp. URL: http://www.res.titech.ac.jp/polymer.

10.1021/jp992172s CCC: $18.00
Published on Web 10/22/1999

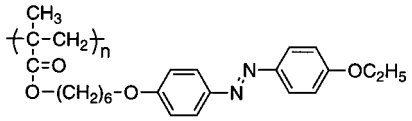

PM6AB2
Mw = 79,000; Mw/Mn = 4.4
G 68 N 150 I

Figure 1. Chemical structure and properties of **PM6AB2** used in this study: G, glass; N, nematic; I, isotropic; M_n, number-average molecular weight; and M_w, weight-average molecular weight.

tion of the refractive index have not fully been discussed because the modulation was very small. As mentioned above, polymer azobenzene liquid-crystal (PALC) is a supramolecular assembly and shows various unique characteristics. In this paper, we report photoinduced formation of the phase-type gratings in PALC.[13h] It was expected that additional properties that could not be observed in the conventional surface-relief gratings would emerge in this study: the light-induced change in the refractive index might become an important factor.

Experimental Section

Materials and Preparation of Films. Chemical structure and physical properties of PALC are shown in Figure 1. **PM6AB2** exhibited the N phase between 68 and 150 °C. To obtain an oriented film, **PM6AB2** was dissolved in tetrahydrofuran (2 mg/mL), and then a small portion of the resultant solution was cast on polyimide-coated glass substrate. Before casting, the substrate was rubbed in a unidirectional way with a clean cloth. An optically transparent and homogeneously aligned film was obtained after annealing the film at a temperature just below the N-to-I phase-transition temperature (T_{NI}) of **PM6AB2**. To confirm unidirectional alignment of the azobenzene moieties in the prepared films, we measured polarized absorption spectra with a UV−vis spectrometer (Japan Spectroscopic Co., model Ubest V-550) and calculated an order parameter; the order parameter was estimated as 0.40−0.50. A thickness of the film was measured as 500−600 nm with a profile measurement microscope (Keyence Co., model VF-7500). It was also confirmed that **PM6AB2** showed no absorption at the wavelength of the readout beam (633 nm). Hence, nondestructive readout was possible.

Optical Setup and Experimental Conditions. Figure 2A illustrates the optical setup for recording of gratings. An unpolarized 488 nm beam from an Ar^+ laser (Laser Drive Inc., model 9600 for laser power supply; National Laser Co., model H61WBLd0AW for laser head) was employed as the writing beams (beams 1 and 2), and two beams obtained with a beam splitter at an equal light intensity were interfered on the film at an incidence angle of θ (Figure 2A). Fringe spacing (Λ) was calculated according to the following equation:

$$\Lambda = \frac{\lambda_W}{2 \sin \theta} \tag{1}$$

where λ_W is the wavelength of the writing beams. The beams were collimated to a diameter of approximately 2 mm on the film. In this study, all experiments were performed in the Raman−Nath (thin) regime, and multiple diffraction beams were observed. Grating formation was evaluated by real-time monitoring of the change in intensity of the first-order diffraction beam at 633 nm from a He−Ne laser (NEC Co., model GLS5360 for the laser power supply; GLG5260 for the laser head).

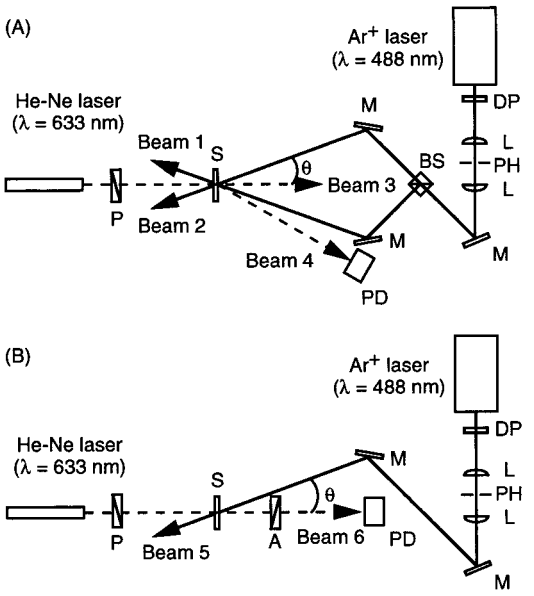

Figure 2. Optical setup for evaluation of formation of holographic diffraction gratings (A) and photochemical phase transition behavior (B). A, analyzer; beams 1 and 2, writing beams; beam 3, 0th-order diffraction beam; beam 4, +first-order diffraction beam; beam 5, pumping beam; beam 6, probe beam; BS, beam splitter; DP, depolarizer; L, lens; M, mirror; P, polarizer; PD, photodiode; PH, pinhole; and S, sample.

Evaluation of the photochemical N-to-I phase-transition behavior of **PM6AB2** was performed with the optical setup shown in Figure 2B. The film was irradiated with an unpolarized beam at 488 nm. Intensity of the linearly polarized beam at 633 nm (beam 6) transmitted through a pair of crossed polarizers, with the film between them, was monitored at various temperatures with a photodiode.

Characterization of Gratings. In this study, the first-order diffraction efficiency (η) was defined as the ratio of the intensity of the first-order diffraction beam (beam 4, I_D) to that of the transmitted beam through the film in the absence of the writing beams:

$$\eta\ (\%) = \frac{I_D}{I_T} \times 100 \tag{2}$$

After the beams were recorded, anisotropy in the diffraction efficiency with respect to polarization of the readout beam was investigated at room temperature. In ordinary experiments, the polarization direction of the readout beam was parallel to the vertical axis ($\alpha = 90°$, Figure 5). In evaluation of the anisotropy, the diffraction efficiency was measured by rotating the polarization of the readout beam at room temperature. Gratings recorded at 80 °C (N phase) were employed as samples: when η reached to a maximum value, the writing beams were switched off, and then, the film was cooled to room temperature.

A recorded interference pattern was observed with a polarizing optical microscope (POM, Olympus, BK50) at room temperature.

Atomic Force Microscope (AFM) Measurements. After grating formation, the surface structure of the polymer films was investigated with an AFM (Seiko Instruments Inc., SPA-400). Gratings were recorded in different phases and at different exposure times. At an appropriate time, the writing beams were turned off, and then, the film was cooled to room temperature, at which the polymer was in glassy state. For each sample, η was estimated by eq 2.

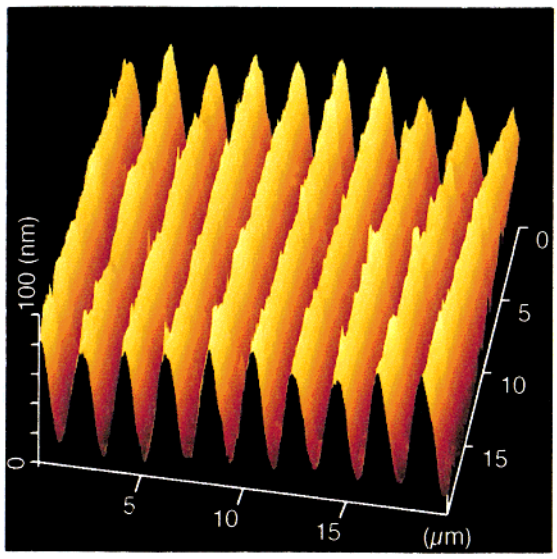

(A)

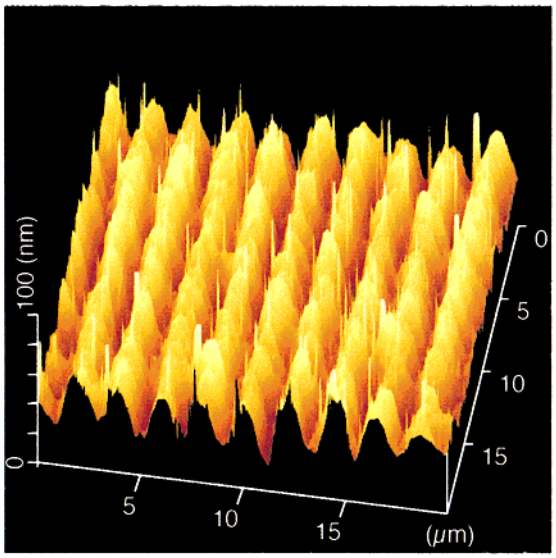

(B)

Figure 3. AFM 3-D views of the gratings recorded in the glassy state (A) and the nematic phase (B). AFM measurements were performed at room temperature. The surface modulation and the diffraction efficiency are listed in Table 1.

Results and Discussion

Surface Structure of the Grating. It has been demonstrated that azobenzene polymers exhibit surface-relief gratings in addition to birefringent gratings on irradiation with two polarized writing beams.[3b,8,9] Although two unpolarized beams were employed for the grating formation in this study, it was presumed that similar surface modulation would be generated on the film. Figure 3 shows typical AFM 3-D views of the gratings recorded in different phases. Table 1 summarizes the surface modulation and the diffraction efficiency. Samples 1 and 2 were recorded in the glassy state (room temperature), and samples 3 and 4 were recorded in the N phase (80 °C). AFM measurements were performed at room temperature. Figure 3A reveals that a very fine relief structure is present on the film. Modulation was between 68 and 76 nm and η was 18% (sample 1). On the other hand, a somewhat distorted relief structure was observed when the grating formation was carried out in the N phase, as shown in Figure 3B. The modulation was between 31 and 34 nm and η was 21% (sample 4). In the surface-relief gratings, the diffraction efficiency is strongly dependent on surface modulation. Actually, the grating with large modulation showed high diffraction efficiency (sample 1) when gratings were recorded at the same temperature. However, almost the same efficiencies were observed for two samples (η = 18 and 21% for samples 1 and 4, respectively), whereas the surface modulation obtained in the glassy state was approximately twice as large as that obtained in the N phase. Furthermore, Table 1 gives another intriguing consequence for the relationship between the surface modulation and the diffraction efficiency. By comparing samples 2 and 4, a three-times larger value was obtained by recording in the N phase, even if the gratings had the same modulation. Previously, Natansohn and co-workers reported that the theoretically calculated diffraction efficiency from the surface modulation (170 nm) was in good agreement with the experimentally obtained value (η = 28%).[9a] In this study, we could acquire the same diffraction efficiency with a modulation of 33−53 nm. This means that the efficiency was enhanced by a factor of 3−5 in the liquid-crystalline phase. To our knowledge, this is the first example of a large enhancement of the diffraction efficiency in the liquid-crystalline phases. Generation of the spatial modulation of the refractive index, which is another type of the phase-type grating, may be contributing to the grating formation.

TABLE 1. Surface Modulation and Diffraction Efficiency (η) of the Gratings Recorded in the Different Phase Structures[a]

sample	phase structure	modulation (nm)	η (%)
1	glassy state	68−76	18
2	glassy state	32−38	7
3	N phase	33−53	28
4	N phase	31−34	21

[a] Each sample was prepared by changing the exposure time.

Dynamics of the First-Order Diffraction Beam. Figure 4 shows typical profiles of the first-order diffraction efficiency as a function of time at various temperatures (line A). The experiments were performed at $\theta = 7°$, corresponding to Λ = 2 μm. Total intensity of the writing beams was 120 mW/cm^2. The diffraction beams, up to the fourth-order diffraction beams, were immediately observed when the writing beams were turned on. Dynamics of the diffraction beam was much influenced by temperature. The response time of the diffraction beam became shorter as temperature increased. The diffraction efficiency reached to its maximum value within several 10 s at these temperatures. This is a much faster response than those previously reported.[8a−d,9b] In the previous studies, very long exposures, at least several hundred of seconds or several minutes, were necessary for the grating formation because large surface modulations must be induced. Faster response is favorable for development of high-sensitivity materials and dynamic holography.

Above T_{NI}, the diffraction beams were hardly observed, even if the writing beams were turned on. This indicates that the grating formation did not result from changes in density or molecular shape. It is suggested that macroscopic changes were induced in the film.

Figure 4 also shows the change in intensity of the probe beam transmitted through crossed polarizers on irradiation of the pumping beam at various temperatures (line B). On exposure of the beam, the transmittance immediately decreased. It was caused by the photochemical N-to-I phase transition of **PM6AB2** due to trans−cis photoisomerization of the azobenzene moiety.[13a,b]

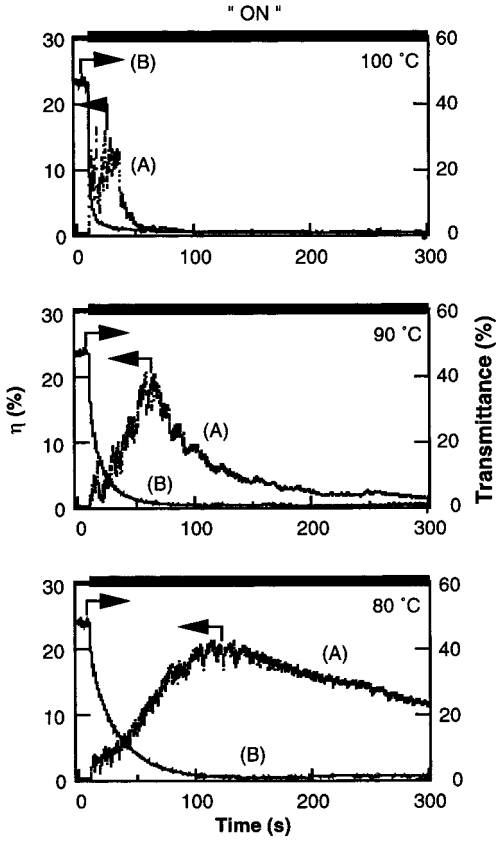

Figure 4. Typical profiles of the first-order diffraction efficiency (A, grating formation) and the transmittance (B, photochemical phase transition) as a function of time at various temperatures. For the grating formation, total intensity of the writing beams was 120 mW/cm^2 and $\Lambda = 2$ μm at $\theta = 7°$. The intensity of the pumping beam was 120 mW/cm^2 for the photochemical phase transition.

This phase transition was also influenced by temperature. It was found that the time necessary to obtain the highest diffraction efficiency almost coincided with the time required for the photochemical N-to-I phase transition at each temperature. We speculated that the I phase was induced photochemically in the bright areas of the interference fringe pattern. It is assumed that this large scale change in the molecular alignment is associated with the grating formation and the enhancement of the diffraction efficiency. In case where that the grating is formed only by the spatial modulation of the refractive index, η can be calculated theoretically by the following equation:

$$\eta = \left(\frac{\pi d \Delta n}{\lambda_R}\right)^2 \tag{3}$$

where d is the film thickness, λ_R is the wavelength of the readout beam, and Δn is the difference in the refractive index between the bright (I phase) and the dark (N phase) areas. From the experimentally obtained value of η, Δn was estimated as 0.150−0.180. In ordinary measurements, the polarization of the readout beam was parallel to the rubbing direction. Hence Δn is represented as $|n_e - n|$, in which n_e denotes the refractive index of LCs for the extraordinary ray and n is the index of the I phase. 4-Butyl-4′-methoxyazobenzene (BMAB, K 30 N 45 I) may be used as a low-molecular-weight model compound because the chemical structure of the azobenzene moiety of BMAB is analogous to that of **PM6AB2**. In the reflection-mode studies,[13g,h] we already measured the indices of BMAB, and Δn ($= |n_e - n|$) was estimated as 0.112−0.156 in the N phase. Our calculated Δn was relatively large compared with the value

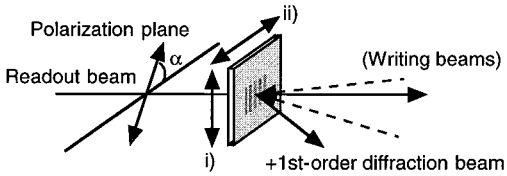

Figure 5. Experimental configuration for evaluation of the anisotropy in the diffraction efficiency. Symbol α denotes the direction of polarization of the readout beam. The direction of the polarization is parallel to vertical axis at $\alpha = 90$ and 270°. Symbols *i* and *ii* denote the rubbing directions.

estimated from BMAB. It is, however, evident that the spatial modulation of the refractive index largely contributes to the grating formation.

Effect of Polarization of Readout Beam on Diffraction Efficiency. Todorov and co-workers explored the diffraction efficiency and its dependence on polarization of readout beam for gratings produced in poly(vinyl alcohol) doped with methyl orange.[1c] They reported that the efficiency depends strongly on the polarization of the readout beam.[1c,d] We can expect that the same anisotropy would be obtained in the present system. Figure 5 shows the experimental configuration used for evaluation of the anisotropy. The linearly polarized readout beam is incident on the sample at normal, and the polarization direction of the beam has an angle to the horizontal axis. In Figure 5, the symbols *i* and *ii* denote rubbing directions. In the rubbing direction *i*, a relation of $\alpha = 90$ and 270° means that the polarization direction is parallel to the rubbing direction, as well as parallel to the grooves. On the other hand, the polarization is perpendicular to the rubbing direction at $\alpha = 0$, 180, and 360°. Figure 6i shows experimental results obtained for rubbing direction *i*. It is clearly seen that the diffraction efficiency showed strong anisotropy with respect to the polarization direction of the readout beam. The diffraction efficiency showed the maximum value at $\alpha = 90$ and 270° and the minimum value at $\alpha = 0$, 180, and 360°. Such anisotropy has not been reported in the study of surface-relief gratings. Therefore, we can conclude that this is caused by the spatial modulation of the molecular alignment. Even though the relief structure was formed on the film, the grating would be also made up by alternate arrangement of the N and the I phases. As shown in Figure 7, two phases may be present periodically under the relief structure.

The diffraction of the linearly polarized readout beam occurs on the basis of Δn as well as the surface modulation. It is well-known that general LCs, such as 4-pentyl-4′-cyanobiphenyl and BMAB, show the following relationship:

$$n_e > n > n_o$$

and Δns can be expressed as

$$|n_e - n| > |n_o - n| \tag{4}$$

where n_o is the refractive index of LCs for the ordinary ray. By taking the relationship of eq 4 into consideration, it is expected that the diffraction efficiency is larger with $|n_e - n|$ than it is with $|n_o - n|$ in eq 3. In Figure 6i, the readout beam was diffracted on the basis of $\Delta n = |n_e - n|$ at $\alpha = 90$ and 270° and in terms of $\Delta n = |n_o - n|$ at $\alpha = 0$, 180, and 360°. Actually, larger values were obtained at $\Delta n = |n_e - n|$. This result obviously indicates that the N phase is preserved in the dark areas. Recently, similar results were reported by Simoni and co-workers in dye-doped polymer-dispersed LCs.[2b] They speculated that this anisotropy would originate from photoalignment

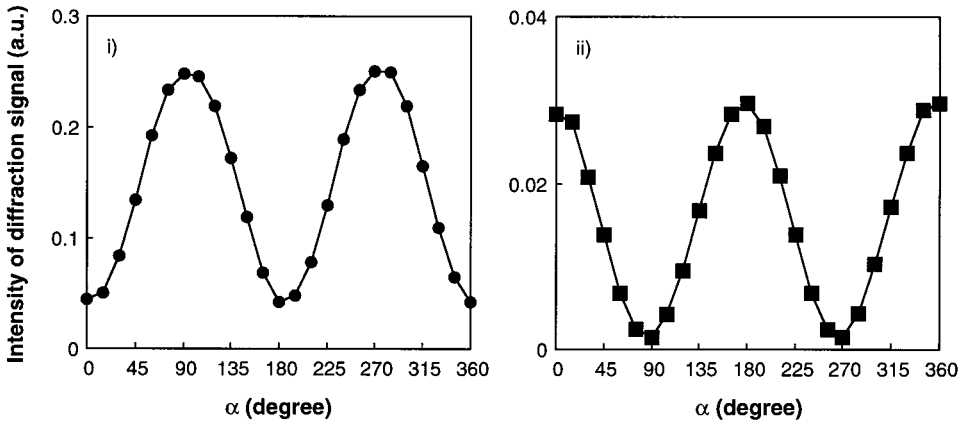

Figure 6. Anisotropy in the diffraction efficiency at different rubbing directions. Symbols *i* and *ii* denote the rubbing directions described in Figure 5. Measurements were performed at room temperature. When the diffraction efficiency reached the maximum value, the writing beams were switched off, and the film was cooled to room temperature ($<T_g$).

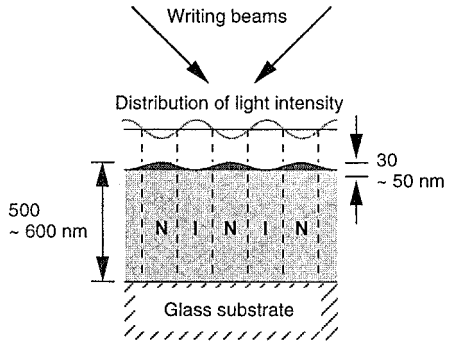

Figure 7. Plausible structure of the holographic diffraction grating. The alternate arrangement of N and I phases is present under the relief structure.

TABLE 2. Differences in the Refractive Indices (Δn) at Each α in the Different Rubbing Directions

	Δn	
rubbing direction	α = 0, 180, and 360°	α = 90 and 270°
i	$\lvert n_o - n \rvert$	$\lvert n_e - n \rvert$
ii	$\lvert n_e - n \rvert$	$\lvert n_o - n \rvert$

of LC droplets containing dye molecules in the bright areas. They also showed the plausible grating structure comprising ordered and disordered alignment.

Effects of Director of N Phase in the Initial State. Next, we investigated the effects of the initial molecular alignment of azobenzene moieties on the anisotropy in the diffraction efficiency. By changing the rubbing direction from *i* to *ii* (Figure 5), the director of the liquid-crystalline phase in the initial state was rotated by 90°, which was confirmed by polarized absorption spectroscopy of the films. In Figure 5, if the diffraction is governed only by surface modulation, the anisotropy must be unchanged by altering the rubbing direction, because gratings with the same grating vector should be formed even if the initial molecular alignment is altered. In other words, the director of liquid-crystalline phase in the initial state would not affect the anisotropy in the diffraction efficiency. Figure 6ii depicts the anisotropy in the efficiency in the rubbing direction *ii*. It is obvious that the profile of the anisotropy is shifted by changing the director in the initial state. Table 2 shows Δn at each α in the rubbing directions *i* and *ii*. As is apparent from Figure 6 and Table 2, the maximum diffraction efficiency was obtained invariably at $\Delta n = |n_e - n|$ in each rubbing direction. These results demonstrate that our consideration for the grating structure shown in Figure 7 is reasonable. Furthermore, the contribution of the periodic modulation in the refractive index to the diffraction efficiency would be dominant, rather than that of surface modulation.

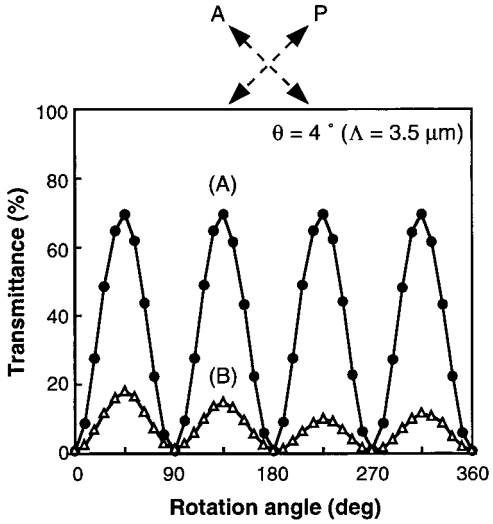

Figure 8. Angular-dependent transmittance of **PM6AB2** film evaluated by polarizing optical microscopy before (A) and after (B) grating experiments.

Observation of Recorded Gratings. Observation of the recorded interference pattern with POM provided conclusive evidence for the grating structure. As viewed through crossed polarizers, transmittance from a homogeneously aligned film is dependent on the rotation angle. When the director is tilted by 45° with respect to the polarizer (P) or analyzer (A), the film is seen as bright. Figure 8 shows the angular-dependent transmittance of the film evaluated by POM before (A) and after (B) exposure to the writing beams. The experiment was conducted at $\theta = 4°$ ($\Lambda = 3.5$ μm). Before exposure, the transmitted light intensity was highest at 45 and 135° and so on, at every 90°, and lowest at 0 and 90° and so on, at every 90°. This indicates that the azobenzene moieties are unidirectionally aligned, i.e., monodomain. After exposure to the writing beams, the same angular dependency of transmittance was obtained. However, the highest intensity of transmittance decreased. Figure 9 shows photographs of the recorded pattern which were viewed through POM. The grating structure was clearly observed at 45 and 135° and so on, at every 90°. On the other hand, it was difficult to observe the grating structure at 0 and 90° and so on, at every 90°. From these findings, it was confirmed that the I phase was induced periodically in the bright

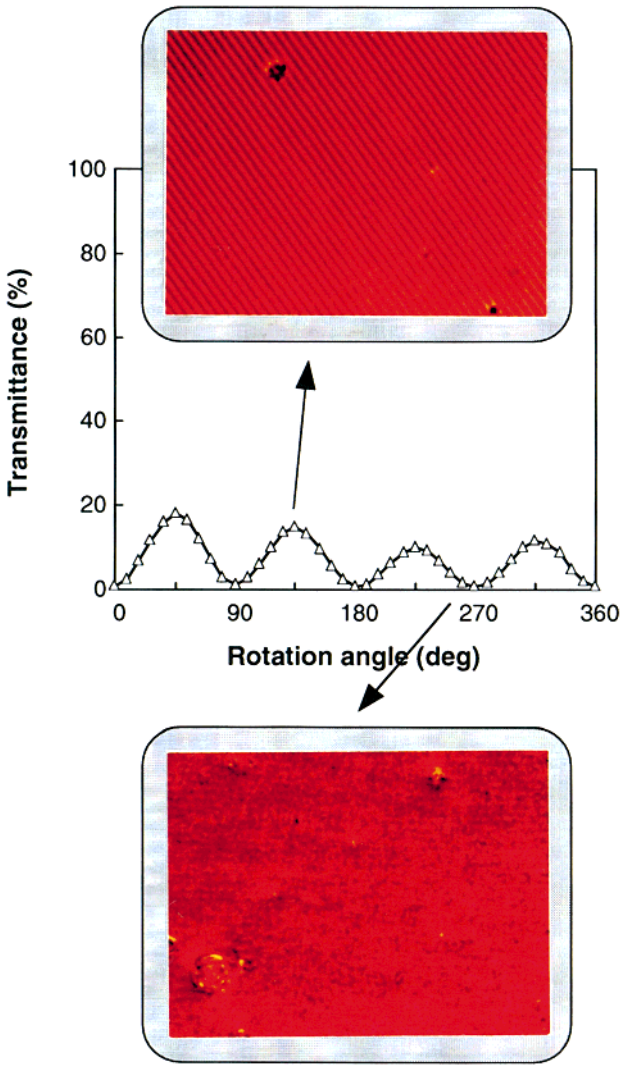

Figure 9. Grating structure recorded in the **PM6AB2** film viewed through crossed polarizers in a polarizing optical microscope. Grating was recorded at $\theta = 4°$ ($\Lambda = 3.5$ μm).

areas of the interference pattern (the dark regions in Figure 9), and the N phase was preserved in the dark areas (the bright regions).

Conclusion

We explored the formation of phase-type gratings in **PM6AB2** films. AFM measurements revealed that the slight surface modulation was formed on the film, when the grating formation was carried out in the N phase. Large enhancement in the diffraction efficiency and the faster response were observed under appropriate conditions. It is considered that these results are attributed to the spatial modulation of the refractive index. The grating formation resulted from the photochemical N-to-I phase transition of **PM6AB2**. It was found that the gratings consisted both of the spatial modulation of the surface structure and of the periodic arrangement of N and I phases. Strong anisotropy was observed in the diffraction efficiency with respect to polarization of the readout beam. This indicates that the spatial modulation of the refractive index, which resulted from the periodic induction of the photochemical phase transition, would mainly contribute to the grating formation. We could prepare a novel type of phase-type gratings that arise from the photochemical reaction of azobenzene moieties. PALC would be useful for holography and various applications.

References and Notes

(1) (a) Todorov, T.; Tomova, N.; Nikolova, L. *Opt. Commun.* **1983**, *47*, 123−126. (b) Todorov, T.; Nikolova, L.; Tomova, N. *Appl. Opt.* **1984**, *23*, 4309−4312. (c) Todorov, T.; Nikolova, N.; Tomova, N. *Appl. Opt.* **1984**, *23*, 4588−4591. (d) Nikolova, L.; Todorov, T. *Opt. Acta* **1984**, *31*, 579−588. (e) Todorov, T.; Nikolova, L.; Stoyanova, K.; Tomova, N. *Appl. Opt.* **1985**, *24*, 785−788.

(2) (a) Simoni, F.; Francescangeli, O.; Reznikov, Y.; Slussarenko, S. *Opt. Lett.* **1997**, *22*, 549−551. (b) Cipparrone, G.; Mazzulla A.; Simoni, F. *Opt. Lett.* **1998**, *23*, 1505−1507.

(3) (a) Hvilsted, S.; Andruzzi, F.; Kulinna, C.; Siesler, H. W.; Ramanujam, P. S. *Macromolecules* **1995**, *28*, 2172−2183. (b) Ramanujam, P. S.; Holme, N. C. R.; Hvilsted, S. *Appl. Phys. Lett.* **1996**, *68*, 1329−1331. (c) Rasmussen, P. H.; Ramanujam, P. S.; Hvilsted, S.; Berg, R. H. *J. Am. Chem. Soc.* **1999**, *121*, 4738−4743.

(4) Martin, S.; Feely, C. A.; Toal, V. *Appl. Opt.* **1997**, *36*, 5757−5768.

(5) Kohler, B.; Bernet, S.; Renn, A.; Wild, U. P. *Opt. Lett.* **1993**, *18*, 2144−2146.

(6) Akella, A.; Sochava, S. L.; Hesselink, L. *Opt. Lett.* **1997**, *22*, 919−921.

(7) (a) Eich, M.; Wendorff, J. H. *Makromol. Chem., Rapid Commun.* **1987**, *8*, 59−63. (b) Eich, M.; Wendorff, J. H. *Makromol. Chem., Rapid Commun.* **1987**, *8*, 467−471. (c) Eich, M.; Wendorff, J. H. *J. Opt. Soc. Am. B* **1990**, *7*, 1428−1436. (d) Anderle, K.; Wendorff, J. H. *Mol. Cryst. Liq. Cryst.* **1994**, *243*, 51−75.

(8) (a) Kim, D. Y.; Li, L.; Jiang, X. L.; Shivshankar, V.; Kumar, J.; Tripathy, S. K. *Macromolecules* **1995**, *28*, 8835−8839. (b) Jiang X. L.; Li, L.; Kumar, J.; Kim, D. Y.; Shivshankar, V.; Tripathy, S. K. *Appl. Phys. Lett.* **1996**, *68*, 2618−2620. (c) Kim, D. Y.; Lee, T. S.; Tripathy, S. K.; Jiang, X. L.; Li, L.; Kumar, J. *Macromol. Symp.* **1997**, *116*, 127−134. (d) Lee, T. S.; Kim, D. Y.; Jiang, X. L.; Li, L.; Kumar, J.; Tripathy, S. K. *J. Polym. Sci., Part A: Polym. Chem.* **1998**, *36*, 283−289. (e) Kumar, J.; Li, L.; Jiang, X. L.; Kim, D. Y.; Lee, T. S.; Tripathy, S. *Appl. Phys. Lett.* **1998**, *72*, 2096−2098. (f) Jiang, X. L.; Li, L.; Kumar, J.; Kim, D. Y.; Tripathy, S. K. *Appl. Phys. Lett.* **1998**, *72*, 2502−2504.

(9) (a) Rochon, P.; Batalla, E.; Natansohn, A. *Appl. Phys. Lett.* **1995**, *66*, 136−138. (b) Barrett, C. J.; Natansohn, A. L.; Rochon, P. L. *J. Phys. Chem.* **1996**, *100*, 8836−8842. (c) Rochon, P.; Natansohn, A.; Callender, C. L.; Robitaille, L. *Appl. Phys. Lett.* **1997**, *71*, 1008−1010.

(10) (a) Khoo, I. C.; Li, H.; Liang, Y. *Opt. Lett.* **1994**, *19*, 1723−1725. (b) Khoo, I. C. *Opt. Lett.* **1995**, *20*, 2137−2139. (c) Khoo, I. C.; Slussarenko, S.; Guenther, B. D.; Shih, M. Y.; Chen, P.; Wood, W. V. *Opt. Lett.* **1998**, *23*, 253−255.

(11) (a) Ono, H.; Kawatsuki, N. *Jpn. J. Appl. Phys.* **1997**, *36*, 6444−6448. (b) Ono, H.; Kawatsuki, N. *Appl. Phys. Lett.* **1997**, *71*, 1162−1164.

(12) (a) Wiederrecht, G. P.; Yoon, B. A.; Wasielewski, M. R. *Science* **1995**, *270*, 1794−1797. (b) Wiederrecht, G. P.; Yoon, B. A.; Svec, W. A.; Wasielewski, M. R. *J. Am. Chem. Soc.* **1997**, *119*, 3358−3364. (c) Wiederrecht, G. P.; Wasielewski, M. R. *J. Am. Chem. Soc.* **1998**, *120*, 3231−3236.

(13) (a) Ikeda, T.; Tsutsumi, O. *Science* **1995**, *268*, 1873−1875. (b) Tsutsumi, O.; Shiono, T.; Ikeda, T.; Galli, G. *J. Phys. Chem. B* **1997**, *101*, 1332−1337. (c) Tsutsumi, O.; Demachi, Y.; Kanazawa, A.; Shiono, T.; Ikeda, T.; Nagase, Y. *J. Phys. Chem. B* **1998**, *102*, 2869−2874. (d) Tsutsumi, O.; Kitsunai, T.; Kanazawa, A.; Shiono, T.; Ikeda, T. *Macromolecules* **1998**, *31*, 355−359. (e) Shishido, A.; Tsutsumi, O.; Kanazawa, A.; Shiono, T.; Ikeda, T.; Tamai, N. *J. Am. Chem. Soc.* **1997**, *119*, 7791−7796. (f) Shishido, A.; Tsutsumi, O.; Kanazawa, A.; Shiono, T.; Ikeda, T.; Tamai, N. *J. Phys. Chem. B* **1997**, *101*, 2806−2810. (g) Lee H. K.; Kanazawa, A.; Shiono, T.; Ikeda, T.; Fujisawa, T.; Aizawa, M.; Lee B. *Chem. Mater.* **1998**, *10*, 1402−1407. (h) Hasegawa, M.; Yamamoto, T.; Kanazawa, A.; Shiono, T.; Ikeda, T. *Adv. Mater.* **1999**, *11*, 675−677. (i) Wu, Y.; Demachi, Y.; Tsutsumi, O.; Kanazawa, A.; Shiono, T.; Ikeda, T. *Macromolecules* **1998**, *31*, 349−354. (j) Wu, Y.; Demachi, Y.; Tsutsumi, O.; Kanazawa, A.; Shiono, T.; Ikeda, T. *Macromolecules* **1998**, *31*, 1104−1108. (k) Wu, Y.; Demachi, Y.; Tsutsumi, O.; Kanazawa, A.; Shiono, T.; Ikeda, T. *Macromolecules* **1998**, *31*, 4457−4463. (l) Wu, Y.; Ikeda, T.; Zhang Q. *Adv. Mater.* **1999**, *11*, 300−302.